Journal of Magnetics 7(3), 63-71 (2002)

Magnetotransport Properties of Co-Fe/Al-O/Co-Fe Tunnel Junctions Oxidized with Microwave Excited Plasma

Kazuhiro Nishikawa[1,3,*], Satoshi Ogata[2,4], Toshihiro Shoyama[2], Wan-Sick Cho[2,5], Tae-Sick Yoon[2,5], Masakiyo Tsunoda[2] and Migaku Takahashi[1,2,*]

[1]*New Industry Creation Hatchery Center, Tohoku University, Aobayama 05, Sendai 980-8579, Japan*
[2]*Department of Electronic Engineering, Graduate School of Engineering, Tohoku University, Aobayama 05, Sendai 980-8579, Japan*
[3]*Production Technology Development Center, SHARP Corporation, Tenri 632-8567, Japan*
[4]*Vaccum Engineering Division, Tsukishima Kikai Co. Ltd., Tsukuda, Tokyo 104-0051, Japan*
[5]*Research Center for Advanced Magnetic Materials, Chungnam National University, Daejeon 305-764, Korea*

(Received 2 August 2002)

Three fabrication techniques for forming thin barrier layer with uniform thickness and large barrier height in magnetic tunnel junction (MTJ) are discussed. First, the effect of immiscible element addition to Cu layer, a high conducting layer generally placed under the MTJ, is investigated in order to reduce the surface roughness of the bottom ferromagnetic layer, on which the barrier is formed. The Ag addition to the Cu layer successfully realizes the smooth surface of the ferromagnetic layer because of the suppression of the grain growth of Cu. Second, a new plasma source, characterized as low electron energy of 1 eV and high density of 10^{12} cm^{-3}, is introduced to the Al oxidation process in MTJ fabrication in order to reduce damages to the barrier layer by the ion-bombardment. The magnetotransport properties of the MTJs are investigated as a function of the annealing temperature. As a peculiar feature, the monotonous decrease of resistance area product (*RA*) is observed with increasing the annealing temperature. The decrease of the *RA* is due to the decrease of the effective barrier width. Third, the influence of the mixed inert gas species for plasma oxidization process of metallic Al layer on the tunnel magnetoresistance (TMR) was investigated. By the use of Kr-O_2 plasma for Al oxidation process, a 58.8% of MR ratio was obtained at room temperature after annealing the junction at 300 °C, while the achieved TMR ratio of the MTJ fabricated with usual Ar-O_2 plasma remained 48.4%. A faster oxidization rate of the Al layer by using Kr-O_2 plasma is a possible cause to prevent the over oxidization of Al layer and to realize a large magnetoresistance.

Key words : Annealing temperature dependence, Electrode material, Inert gas, Magnetic tunnel junction, Plasma source.

1. Introduction

Since the discovery of large tunnel magnetoresistance (TMR) over 10% at room temperature [1, 2], a great deal of attention has been focused on the magnetic tunnel junctions (MTJs) because of its possible application for magnetic random access memories (MRAMs). In order to attain a large TMR, that is the key property of MTJs for MRAM application, it is essentially required to realize a very thin barrier layer with uniform thickness and large barrier height [3].

The smooth surface of the ferromagnetic layer is one of the indispensable factors to form homogeneous tunnel barrier on it without pinholes. The surface morphology of high conducting layer, placed under the MTJ to lower the resistance of the electrode, strongly affects the surface roughness of the ferromagnetic layer. Cu as the high conducting layer provides a relatively smooth surface of the ferromagnetic layer, comparing to Al [4]; however, a certain roughness remains. There is room for further material research for the high conducting layer.

Another important factor is the fabrication technique of the barrier layer itself. Up to the present, the most promising method to form the high quality barrier layer is a plasma oxidation process after the deposition of an ultrathin metallic Al layer. By using this method, MTJs with large TMR in excess of 40% have been obtained [5-

*Corresponding author: Fax: +81-22-217-7134, e-mail: migac34@ec.ecei.tohoku.ac.jp/nisikawa@ptlab.tnr.sharp.co.jp

8]. However, in general, plasma oxidation process may introduce some defects in the barrier layer due to the high-energy ion bombardment from the plasma to the specimens [9]. When there exist some defects in the barrier layer of the MTJs, electrons can tunnel the barrier via defect states, and such two step tunneling process [10] lowers the MR ratio and bias voltage, V_h, at which the MR ratio decreases to its half value [11]. Since the ion-bombarding energy strongly depends on the space potential of plasma, which is mainly determined by the electron temperature, one can expect to provide the Al-O layer without introducing any defects, by using an oxidizing plasma with a low electron temperature.

The other factor should be controlled in the plasma oxidation process is the inert gas species. The experimental parameters, such as the applied power to discharge plasma, oxidation time, and operating gas pressure, are generally varied to optimize the oxidation conditions. However, particular attention has not been paid for the role of the inert gas which is usually mixed with oxygen to maintain the plasma discharge stably. As several properties, such as ionizing energy, energy levels of metastable states, and collision cross-sections, are different among the inert gas species, one can expect the change of oxidation process of metallic Al layer by changing the inert gases. In the field of metal oxide semiconductor fabrication, it is known that the electric properties of thin gate insulating layer, fabricated by plasma oxidation of Si, are strongly affected by the inert gases mixed in the oxygen plasma. Kr as a mixed inert gas provides excellent electric properties of the gate oxidation layer, such as lower interface trap density at SiO_2/Si interface, comparing to the case in which Ar gas is used [12, 13].

In this article, we discuss (1) the effects of elements added into Cu of the high conducting layer on the surface roughness of the ferromagnetic layer in MTJs, (2) the magnetotransport properties of the MTJs, the barrier layer of which are oxidized by using a newly developed low electron temperature plasma source, and (3) the influence of the inert gas species on MTJ properties, which are mixed with oxygen in the plasma oxidation process.

2. Experimental Procedure

MTJs with the structure of sub./Ta 50 Å/Cu 200 Å/Ta 200 Å/Ni-Fe 20 Å/Cu 50 Å/$Mn_{75}Ir_{25}$ 100 Å/$Co_{70}Fe_{30}$ 25 Å/Al-O/$Co_{70}Fe_{30}$ 25 Å/Ni-Fe 100 Å/Ta 350 Å/Cu 4000 Å/Ta 50 Å were patterned by photolithographic process and ion milling to the micro junction of 36 μm^2~3600 μm^2. Some MTJs were patterned by metal masks with the structure of sub./Ta 50 Å/Cu 1000 Å/Ta 50 Å/Ni-Fe 20 Å/Cu 50 Å/$Mn_{75}Ir_{25}$ 100 Å/$Co_{70}Fe_{30}$ 25 Å/Al-O/$Co_{70}Fe_{30}$ 25 Å/Ni-Fe 100 Å/Cu 1000 Å with junction area of about 4×10^4 μm^2. As the resistances of all MTJs are large enough compared to the resistance of top and bottom electrical lead, the electrical properties are measured without geometrical influence [14].

All the metallic films were deposited by dc magnetron sputtering method in the chamber having the base pressure of 3×10^{-9} Torr using highly purified (9N) Ar gas. The barrier formation was performed by depositing a 15-Å-thick metallic Al film and subsequently oxidizing it in the oxidation chamber having a radial line slot antenna (RLSA).

Figure 1(a), (b) illustrates a RLSA and a oxidation chamber using a RLSA, respectively [15-17]. The RLSA, a microwave-guide planar array, consists of two metal disks separated by a dielectric plate and the top one has many slot pairs which are the unit radiators of microwave. 2.45 GHz microwave is introduced through a coaxial waveguide and the microwave power is radiated from the slots into the vacuum chamber through the quartz window. A low electron temperature of 1 eV and high-density plasma of 10^{12} cm^{-3} is obtained at the substrate position, 50 mm distant from the quartz window [18].

He, Ar, and Kr were used as the inert gases mixed with O_2 molecule gas for the plasma oxidation. The standard

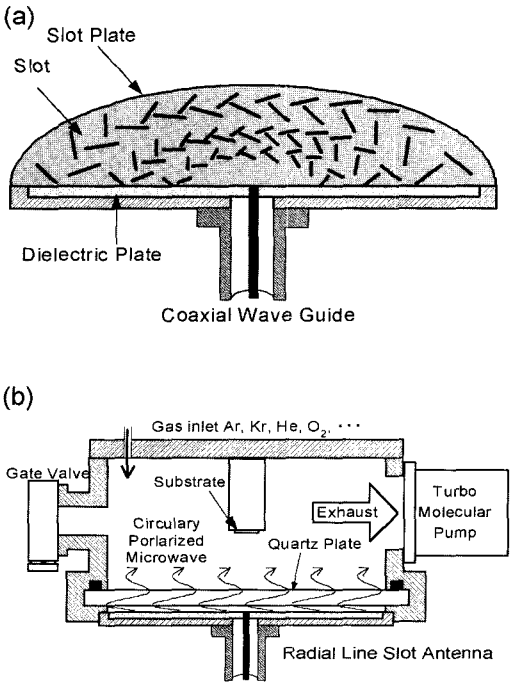

Fig. 1. Schematic illustration of (a) a radial line slot antenna (RLSA) and (b) newly introduced plasma oxidation chamber using a RLSA.

condition of operating pressure of the mixed gas and the O_2 concentration in it were 1 Torr and 3%, respectively. The applied microwave power density was 1.1 W/cm^2. The oxidation time was varied from 3.5 to 40 s. The thermal treatment consists of consecutive 60 min vacuum annealing at each temperature, followed by furnace field cooling.

3. Result and Discussion

3.1. Electrode material for smooth surface of bottom ferromagnetic layer

The surface morphology of the ferromagnetic layer, on which the barrier Al-O layer is formed, generally traces that of the high conducting Cu layer. Therefore, the suppression of grain growth in the Cu layer is effective to obtain the smooth surface of ferromagnetic layer. We can expect to suppress the grain growth of Cu layer by adding immiscible element with Cu.

For this investigation, the samples with the structure of Ta 50 Å/X *d*/Ta 50 Å/Ni-Fe 20 Å/X 50 Å/$Mn_{75}Ir_{25}$ 100 Å/$Co_{70}Fe_{30}$ 25 Å were prepared on the thermally oxidized Si wafer. Cu, $Cu_{96.4}Ta_{3.6}$, $Cu_{96.4}W_{3.6}$, $Cu_{91.6}Ag_{8.4}$ were investigated as material X and the thickness *d* was ranged 0 to 1000 Å.

Figure 2 shows the AFM images of the top surface (corresponding to the surface of the bottom ferromagnetic layer in MTJ) of as-deposited samples with X = Cu and (a) *d* = 0 Å, (b) *d* = 1000 Å, for example. With increasing the thickness, *d*, the surface morphology drastically changes. Surface roughness, R_a are determined for all the samples from the AFM measurements. Figure 3(a) shows the surface roughness, R_a of the samples with X = Cu, Cu-Ta, Cu-W, and Cu-Ag as a function of the electrode thickness, *d*. Independent of the material X, R_a increases with increasing *d*. However, there is a large difference of R_a among the samples having different material (X) when the electrode thickness (*d*) is set at the same value. The surface roughness of the samples with X = Cu-Ta, Cu-W, and Cu-Ag are clearly smaller than that of the samples with X = Cu. On the other hand, the sheet resistance of the samples largely increased by changing the electrode material from Cu to Cu-Ta or Cu-W. The sheet resistance of the sample with X = Cu-Ta was 6.2 Ω/square, while that of the sample with X = Cu was 0.3 Ω/square at *d* = 1000 Å. We thus compare the R_a of the samples under the same sheet resistance. Figure 3(b) shows the relation between R_a and sheet resistance of the samples with X = Cu, Cu-Ta, Cu-W, and Cu-Ag. The R_a of the samples with X = Cu-Ta or Cu-W are larger than that of the sample with X = Cu. On the other hand, the R_a of the sample with X = Cu-Ag are smaller than that of the sample with X = Cu at the same sheet resistance. In addition, we have otherwise confirmed the surface roughness of the samples with X = Cu-Ag isn't enlarged even after the thermal annealing at 300 °C. This means that Cu-Ag electrode is

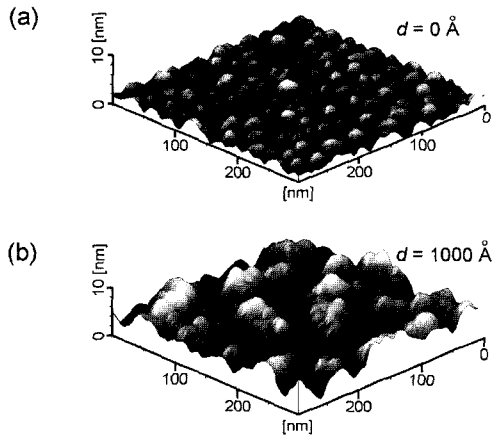

Fig. 2. AFM topographic images of the samples with the structure of Ta 50 Å/Cu *d*/Ta 50 Å/Ni-Fe 20 Å/Cu 50 Å/$Mn_{75}Ir_{25}$ 100 Å/$Co_{70}Fe_{30}$ 25 Å. The thickness *d* is (a) 0 Å, and (b) 1000 Å, respectively.

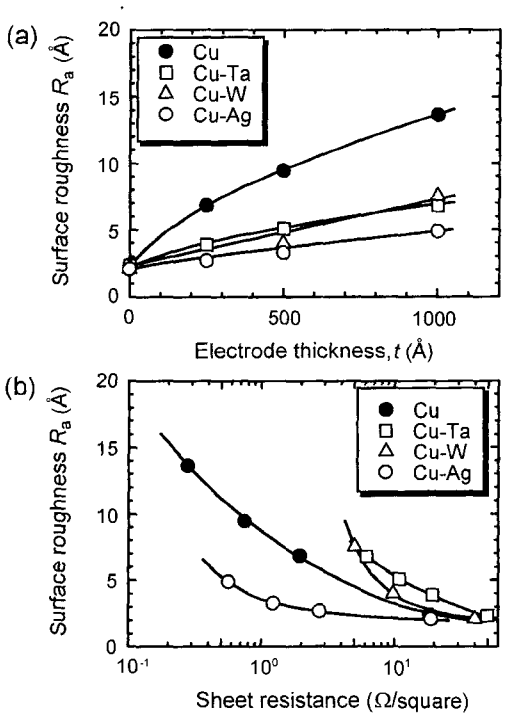

Fig. 3. Surface roughness of the samples with the structure of Ta 50 Å/X *d*/Ta 50 Å/Ni-Fe 20 Å/X 50 Å/$Mn_{75}Ir_{25}$ 100 Å/$Co_{70}Fe_{30}$ 25 Å as a function of (a) electrode thickness and (b) sheet resistance. Cu, $Cu_{96.4}Ta_{3.6}$, $Cu_{96.4}W_{3.6}$, $Cu_{91.6}Ag_{8.4}$ are used as material X and the thickness *d* is ranged 0 to 1000 Å.

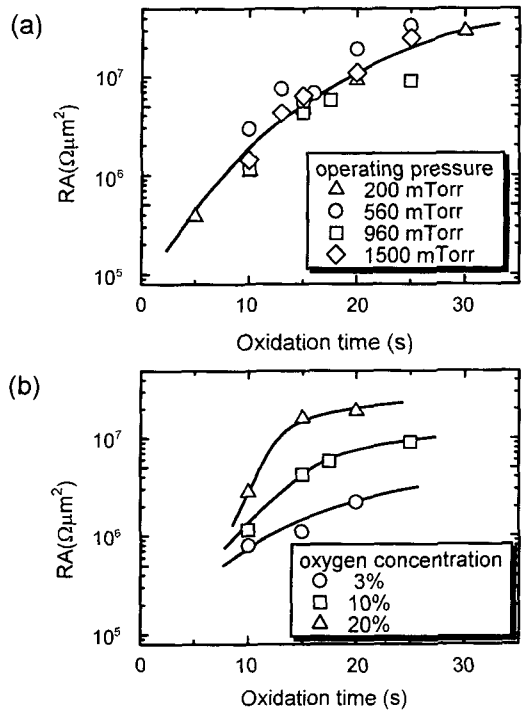

Fig. 4. Oxidation time dependence of resistance-area (*RA*) product of the MTJs patterned by metal masks with the structure of sub./Ta 50 Å/Cu 1000 Å/Ta 50 Å/Ni-Fe 20 Å/Cu 50 Å/ $Mn_{75}Ir_{25}$ 100 Å/$Co_{70}Fe_{30}$ 25 Å/Al-O/$Co_{70}Fe_{30}$ 25 Å/Ni-Fe 100 Å/Cu 1000 Å. Al-O layers are formed by the plasma oxidation of the 15-Å thick Al layer with (a) the operating pressure of 200~1500 mTorr (oxygen concentration was fixed at 3%) and (b) the oxygen concentration of 3 to 20% (the operating pressure was fixed at 950 mTorr).

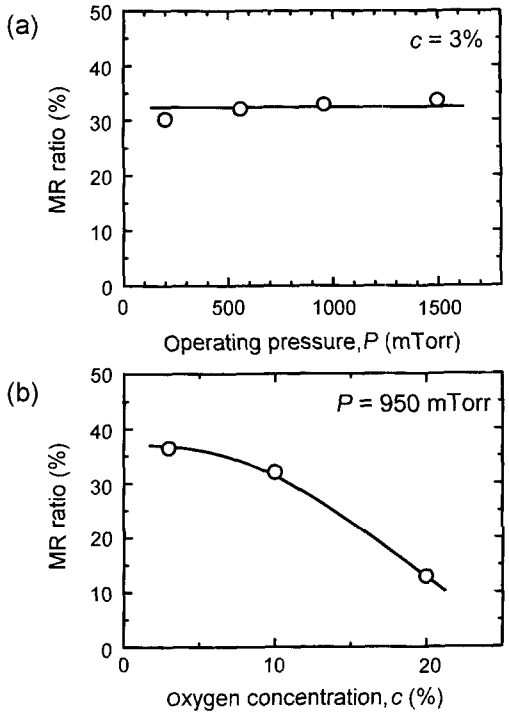

Fig. 5. The MR ratio of the MTJs patterned by metal masks with the structure of sub./Ta 50 Å/Cu 1000 Å/Ta 50 Å/Ni-Fe 20 Å/Cu 50 Å/$Mn_{75}Ir_{25}$ 100 Å/$Co_{70}Fe_{30}$ 25 Å/Al-O/ $Co_{70}Fe_{30}$ 25 Å/Ni-Fe 100 Å/Cu 1000 as a function of (a) the gas pressure and (b) oxygen concentration; The maximum MR ratio obtained during the thermal annealing process up to 300 °C is plotted for the MTJs, having the *RA* of 2×10^6-6×10^6 $\Omega\mu m^2$ in the as prepared state.

favorable to realize the smooth surface of the bottom ferromagnetic layer in MTJs with keeping low sheet resistance.

3.2. Plasma oxidation process for low damage barrier formation

In this section, we show the magnetotransport properties, the barrier layers of which are formed by the Al oxidation using a RLSA microwave plasma. Ar+O_2 mixing gas was used in the oxidation process at this experiment. Figure 4 shows the resistance-area products (*RA*) of as-prepared MTJs as a function of the plasma oxidation time. The results for MTJs oxidized under the condition (a) oxygen concentration, $c = 3\%$ and operating pressure of mixing gas, $P = 200$~1500 mTorr, and (b) $c = 3$~20% and $P = 950$ mTorr. From these figures, we conclude that the oxidation rate is independent on the operating gas pressure while it becomes high with increasing the oxygen concentration.

Figure 5 shows the maximum MR ratio of MTJs obtained during the annealing process up to 300 °C as a function of (a) the operating pressure, P and (b) the oxygen concentration, c. In Fig. 5, the results of the MTJs, having the *RA* of 2×10^6-6×10^6 $\Omega\mu m^2$ in the as prepared state, are plotted. As well as the oxidation rate shown in Fig. 4(a), there is no large dependence of the maximum MR ratio on operating pressure, P, while the maximum MR ratio decreases with increasing the oxygen concentration, c. Taking into account that the plasma discharge is more stable at high operating pressure, we decided the standard oxidation condition as $P = 1$ Torr and $c = 3\%$ for the following experiment.

Figure 6 shows the annealing temperature dependence of MR ratio, *RA* product, barrier height and barrier width for the MTJs, barrier layers of which are formed with Ar + O_2 plasma [19].

The data plotted at 120 °C correspond to those for the as-prepared MTJs. The barrier height and the barrier width were obtained by fitting the current-voltage curves with the Simmons formula [20]. The barrier height and the barrier width are plotted only in the annealing temper-

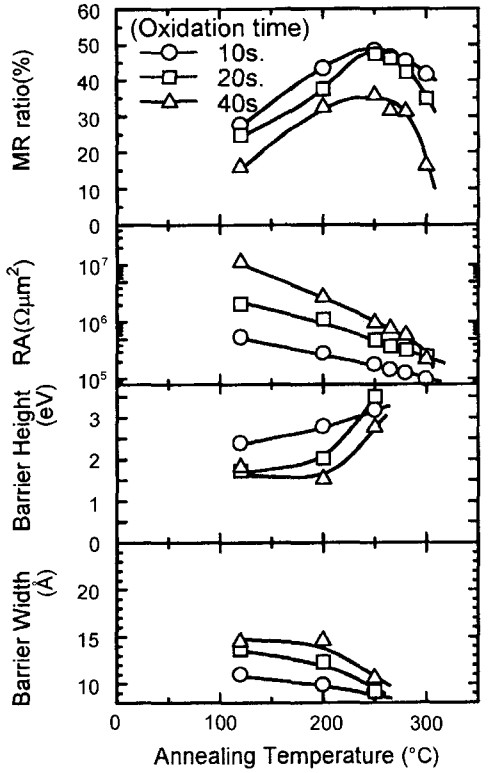

Fig. 6. Annealing temperature dependence of MR ratio, *RA* product, barrier height, and barrier width for the MTJs with the structure of sub./Ta 50 Å/Cu 200 Å/Ta 200 Å/Ni-Fe 20 Å/Cu 50 Å/$Mn_{75}Ir_{25}$ 100 Å/$Co_{70}Fe_{30}$ 25 Å/Al-O/$Co_{70}Fe_{30}$ 25 Å/Ni-Fe 100 Å/Ta 350 Å/Cu 4000 Å/Ta 50 Å. The Al-O layers were formed by the Ar+O_2 plasma oxidation of 15-Å thick Al layers.

ature range where the barrier parameters for both the positive and the negative branches of the current-voltage characteristics are not significantly deviated. For all MTJs, the MR ratio increases by thermal annealing and reaches a peak around the annealing temperature, T_a of 250 °C. The MR ratio of 48.4% is obtained at T_a = 250 °C in the case of the MTJ fabricated with 10 s oxidation time. The V_h of 420 mV, separately measured, for the same MTJ indicates that a good quality barrier is formed with using the RLSA oxidation plasma process. The monotonous decrease of the *RA* product in coincidence with the decrease of the barrier width with increasing the annealing temperature is the peculiar feature for the MTJs fabricated with the RLSA plasma oxidation technique. In the case of the MTJ fabricated by using 10 s oxidation of Al layer with Ar + O_2 plasma, *RA* decreases from 5.4×10^5 $\Omega\mu m^2$ to 1.8×10^5 $\Omega\mu m^2$ and the barrier width decreases from 11 Å to 9 Å with increasing T_a from 120 °C to 250 °C. Even though the oxidation time is changed, the *RA* and the barrier width of MTJs show similar behaviors

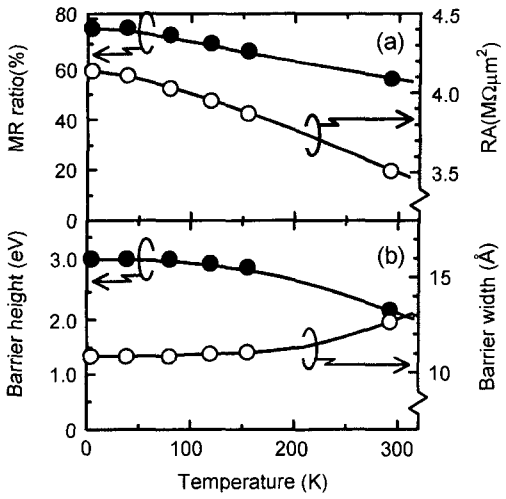

Fig. 7. Measuring temperature dependence of (a) MR ratio and RA product, (b) barrier height and barrier width of the MTJ with the structure of sub./Ta 50 Å/Cu 200 Å/Ta 200 Å/Ni-Fe 20 Å/Cu 50 Å/$Mn_{75}Ir_{25}$ 100 Å/$Co_{70}Fe_{30}$ 25 Å/Al-O/$Co_{70}Fe_{30}$ 25 Å/Ni-Fe 100 Å/Ta 350 Å/Cu 4000 Å/Ta 50 Å after annealed at 300 °C. The Al-O layer was formed by the He+O_2 plasma oxidation of 15-Å thick Al layers for 15 s.

against T_a.

In order to clarify the mechanism of the *RA* decrease with increasing T_a, we investigated the temperature dependence of the magnetotransport properties for the MTJ after thermal annealing [17]. Figure 7 shows the changes of (a) MR ratio and *RA*, (b) barrier height and barrier width, as a function of the measuring temperature, for the MTJ oxidized by He + O_2 plasma and annealed at T_a = 300 °C. The MR ratio increases up to 76% with decreasing the temperature down to 4.2 K. The *RA* and the barrier height increase and the barrier width decreases for decreasing temperature. Taking into account the criteria for tunnel conduction [21], one can say that the conduction of this annealed MTJ is dominated by tunneling and not by pinhole. It means that the decrease of *RA* during thermal annealing is due to the decrease of the insulating barrier thickness. In order to confirm the thinning of the Al-O layer due to the thermal annealing, we estimated the thickness of Al-O layer in the samples before and after annealing by using X-ray reflectivity method. The stacking structure of the sample is sub./Ta 50 Å/Ni-Fe 20 Å/Al-O/Ta 30 Å. Al-O layers are formed by Ar+O_2 plasma after the 100-Å-thick Al layers. Figure 8(a) shows the measured X-ray reflecting profiles of the samples with Al-O layer oxidized for 30 s, for example. Through the fitting of these profiles with the calculated profiles, we determined the Al-O layer thickness. The estimated Al-O thicknesses of the samples as a function of the oxidation

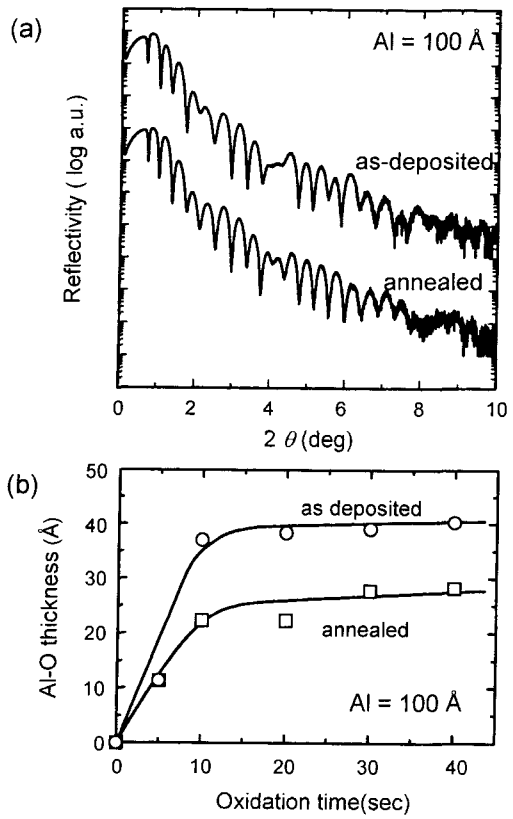

Fig. 8. (a) X-ray reflectivity profiles of the samples, with the structure of sub./Ta 50 Å/Ni-Fe 20 Å/Al-O/Ta 30 Å before and after annealing at 280 °C. Al-O layers are formed by $Ar+O_2$ plasma oxidation of 100-Å-thick Al layer for 30 s. (b) Al-O thickness, determined from the X-ray reflectivity, as a function of oxidation time for the samples with the structure of sub./Ta 50 Å/Ni-Fe 20 Å/Al-O/Ta 30 Å before and after annealing at 280 °C. Al-O layers are formed by $Ar+O_2$ plasma oxidation of 100-Å-thick Al layer.

time are shown in Fig. 8(b). In as deposited samples, Al-O thickness increases with increasing oxidation time up to 10 s, then tends to be saturated about 40 Å. After annealing at 280 °C, the thickness of Al-O layers decreases for nearly 10 Å in the samples oxidized over 10 s.

From these results, we conclude that the changes of the fitted barrier width (Fig. 6) provide a real feature for the changes of the barrier layer structure.

3.3. Effect of inert gas in plasma oxidation process

Figure 9 shows the *RA* product of as-prepared MTJs used three different inert gas for the plasma oxidation process as a function of the oxidation time [22]. In the cases of the junctions fabricated with $He+O_2$ and $Kr+O_2$ plasma, *RA* value increases more rapidly than in the case of the junctions fabricated with $Ar+O_2$ plasma, as the oxidation time increases. It means that the mixing inert

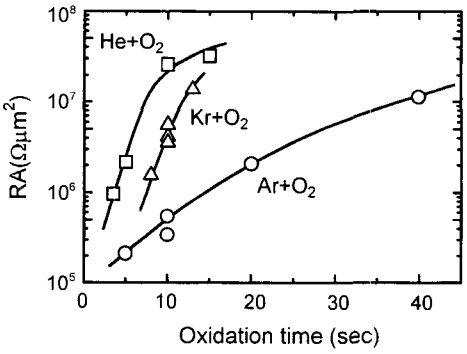

Fig. 9. *RA* product of as prepared MTJs with the structure of sub./Ta 50 Å/Cu 200 Å/Ta 200 Å/Ni-Fe 20 Å/Cu 50 Å/$Mn_{75}Ir_{25}$ 100 Å/$Co_{70}Fe_{30}$ 25 Å/Al-O/$Co_{70}Fe_{30}$ 25 Å/Ni-Fe 100 Å/Ta 350 Å/Cu 4000 Å/Ta 50 Å as a function of oxidation time. Al-O layers are formed by $Ar+O_2$, $He+O_2$, and $Kr+O_2$ plasma oxidation of 15-Å thick Al layers.

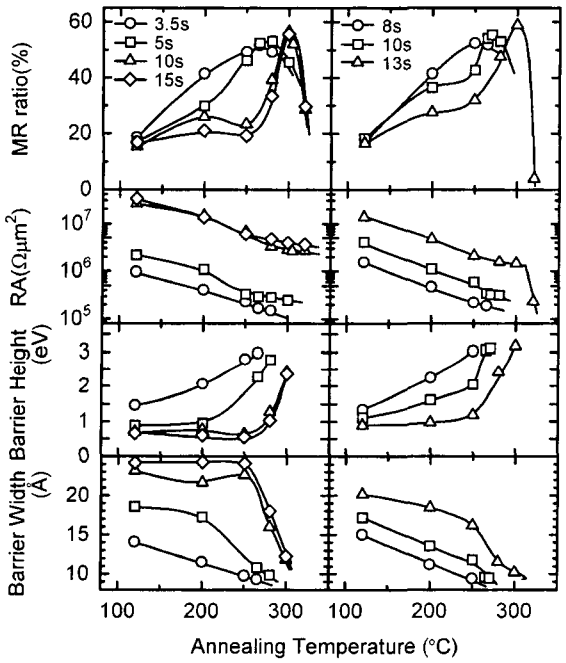

Fig. 10. Annealing temperature dependence of MR ratio, RA product, barrier height, and barrier width for the MTJs with the structure of sub./Ta 50 Å/Cu 200 Å/Ta 200 Å/Ni-Fe 20 Å/Cu 50 Å/$Mn_{75}Ir_{25}$ 100 Å/$Co_{70}Fe_{30}$ 25 Å/Al-O/$Co_{70}Fe_{30}$ 25 Å/Ni-Fe 100 Å/Ta 350 Å/Cu 4000 Å/Ta 50. Al-O layers are formed by $He+O_2$ and $Kr+O_2$ plasma oxidation of 15-Å thick Al layers.

gas species affects the oxidation rate of metallic Al layer. Taking into account the highly efficient generation of $O(2p^4)^1D$ radical by using inert He or Kr rather than Ar [12, 23], one says that the high oxidation rate of metallic Al in $He+O_2$ and $Kr+O_2$ plasma are due to O^1D, which is known as a very active radical.

Figure 10 shows the changes of MR ratio, *RA* and

barrier characteristics of the MTJs, the barrier layers of which are formed using $He+O_2$ or $Kr+O_2$ plasma, as a function of the annealing temperature [22]. The MTJs fabricated with the shortest oxidation times (3.5 s for $He-O_2$ and 8 s for $Kr-O_2$) show a similar behavior as in the case of $Ar+O_2$ (see Fig. 6), in which a maximum MR ratio of nearly 50% is obtained around $T_a = 250$ °C. However, the MTJs fabricated with longer oxidation times show different behaviors. When the oxidation time increases, the annealing temperature where the MR ratio takes maximum shifts to the higher temperature and the achieved MR ratio exceeds 50%. Corresponding to this MR behavior, the barrier parameters for each oxidation time show different trends in their changes against T_a. In general, the barrier height increases with increasing T_a. However, as the oxidation time increases, the annealing temperature at which the barrier height starts to rise clearly shifts to higher temperature. This phenomenon seems to be caused by the penetration of oxygen in the barrier layer during the thermal annealing process. Namely, some amount of oxygen in the barrier layer of the as-prepared samples may loosely bond with Al atoms and migrate within the barrier layer to form a more stable oxide having large barrier height, such as Al_2O_3. The thicker the Al-O layer becomes, as in the as-prepared state fabricated with longer oxidation time, the higher the activation energy is needed for the oxygen to migrate in the barrier layer. Thus the MTJs with longer oxidation times need higher temperature to form the barrier layer with large barrier height. Anyway, in the cases of $He+O_2$ and $Kr+O_2$ plasma, one can obtain a large MR ratio in excess of 50% for MTJs fabricated with longer oxidation time after thermal annealing at 270 °C~300 °C. The maximum value of MR ratio in the present study is 58.8%, obtained in the MTJ fabricated with 13 s oxidation time in $Kr+O_2$ plasma and annealed at $T_a = 300$ °C. This is the largest value which has ever been reported in a Co-Fe/Al-O/Co-Fe tunnel junction system.

In order to know the origin of the larger achievable MR ratio for the cases of $Kr+O_2$ and $He+O_2$ compared with the case of $Ar+O_2$, the maximum MR ratio of each case, fabricated with various oxidation times and treated with the thermal annealing process, is plotted in Fig. 11 as a function of the corresponding *RA* value [22]. A contrastive behavior of MR ratio is found between the $Ar+O_2$ case and the other two cases. The MR ratio of MTJs fabricated with $Ar+O_2$ plasma maintains a value of about 48% when the *RA* is less than 5×10^5 $\Omega\mu m^2$, then decreases to 36% for $RA = 10^6$ $\Omega\mu m^2$ (Fig. 5). On the other hand, for MTJs fabricated with $Kr+O_2$ or $He+O_2$, MR ratio in excess of 50% is obtained at $RA\sim2\times10^5$ $\Omega\mu m^2$ and

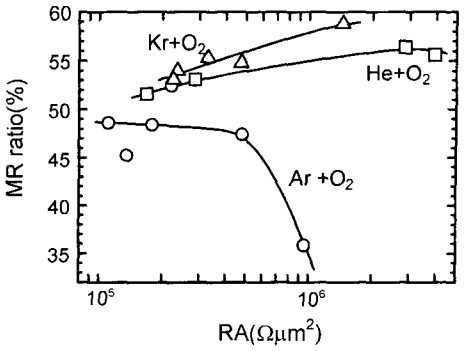

Fig. 11. Plots of the maximum MR ratio obtained in the annealing process vs the corresponding RA product, for the MTJs with the structure of sub./Ta 50 Å/Cu 200 Å/Ta 200 Å/Ni-Fe 20 Å/Cu 50 Å/$Mn_{75}Ir_{25}$ 100 Å/$Co_{70}Fe_{30}$ 25 Å/Al-O/$Co_{70}Fe_{30}$ 25 Å/Ni-Fe 100 Å/Ta 350 Å/Cu 4000 Å/Ta 50. Al-O layers are formed by $Ar+O_2$, $He+O_2$, and $Kr+O_2$ plasma oxidation of 15-Å thick Al layers.

still increases up to $RA > 10^6$ $\Omega\mu m^2$. The cause of the decreasing MR ratio in higher resistance region, found for the $Ar+O_2$ case, is generally explained by the over oxidation mechanism [24, 25]. Namely, the oxidation condition is so strong that the surface of the underlaid ferromagnetic Co-Fe layer is also oxidized and results in the decrease of MR ratio owing to the reduction of the polarization of the ferromagnetic Co-Fe layer. However, the MTJs fabricated with $Kr+O_2$ or $He+O_2$ show larger MR ratio even though they have higher resistance than the over oxidized MTJ with $Ar+O_2$. It means that the over oxidation mechanism was not significant in these MTJs. This result can be explained if we consider the difference of the oxidation process of metallic Al layer with using various mixing inert gases. The oxygen will penetrate to the underlayer surface through the grain boundaries rather than the inner grain of metallic Al layer, because the diffusing mobility of oxygen is generally larger at the grain boundaries than the inner grain. Thus the distribution of the oxygen in MTJs along the film thickness direction will spread as the oxidation time increases, and the underlaid ferromagnetic Co-Fe layer will be oxidized partially. Taking into account the oxidation rate shown in Fig. 9, one says that faster oxidation rate for $Kr+O_2$ or $He+O_2$ case than the $Ar+O_2$ case was favorable to prevent the oxidation of the underlaid ferromagnetic layer and resulted in the large MR ratio even in the high resistance MTJs.

In order to examine this mechanism, we investigated the local current distribution in MTJs using conductive atomic force microscopy (AFM). Figure 12 shows (a) electric current images and (b) line profiles of the electric current measured along the horizontal lines indicated by the

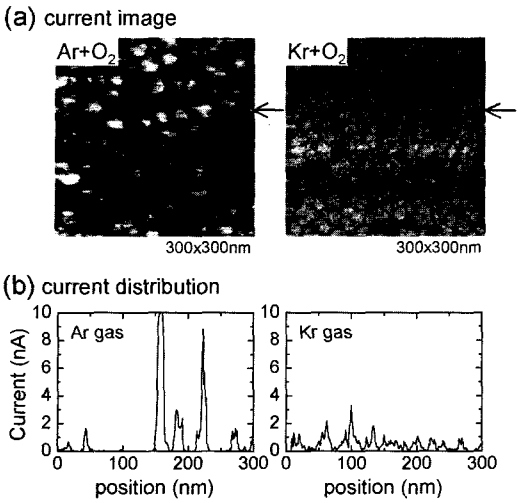

Fig. 12. (a) AFM current images of the samples with the structure of sub./Ta 50 Å/Cu 200 Å/Ta 50 Å/Ni-Fe 20 Å/Cu 50 Å/Mn-Ir 100 Å/$Co_{70}Fe_{30}$ 25 Å/Al-O. The Al-O layers were formed by oxidation of 8-Å-thick Al layer with $Ar+O_2$ plasma for 7 s and $Kr+O_2$ plasma for 3 s. (b) Line profiles of the electric current measured along the horizontal lines indicated by the arrows at right hand side of the current images.

arrows at right-hand side of the current images. The film structure of measured two samples is sub./Ta 50 Å/Cu 200 Å/Ta 50 Å/Ni-Fe 20 Å/Cu 50 Å/Mn-Ir 100 Å/$Co_{70}Fe_{30}$ 25 Å/Al-O. The Al-O layer was formed by oxidation of 8-Å-thick Al layer with $Ar+O_2$ plasma for 7 s and $Kr+O_2$ plasma for 3 s. The oxidation condition is decided for the respective sample to provide the same tunnel resistivity through Al-O layer. In the current images, the bright area corresponds to the area having high tunnel conductance. One can fairly say that the local current distribution of the $Kr+O_2$ oxidation sample is smaller than that of the $Ar+O_2$ oxidation sample. Namely, the $Kr+O_2$ plasma oxidizes the Al layer more uniform than the $Ar+O_2$ plasma.

4. Summary

Three fabrication techniques for forming thin barrier layer with uniform thickness and large barrier height in magnetic tunnel junction (MTJ) are discussed.

1) The effect of immiscible element (Ta, W, Ag) added to Cu layer in MTJ is investigated. The surface roughness of the bottom ferromagnetic layer, on which the barrier layer is formed, is successfully reduced by using $Cu_{91.6}Ag_{8.4}$ for high conducting electrode, instead of Cu.

2) The microwave excited plasma using a RLSA, characterized as low electron temperature of 1 eV and high density of 10^{12} cm^{-3}, is introduced to the Al oxidation process in the MTJ fabrication. The magnetotransport properties of the MTJs are investigated as a function of annealing temperature. As a peculiar feature, the monotonous decrease of *RA* is observed with increasing the annealing temperature of MTJs. It is concluded that the decrease of the *RA* is due to the decrease of the effective barrier width through the examination of measuring temperature dependence on magnetotransport properties of the fabricated MTJ and the change of Al-O thickness by annealing estimated from X-ray reflectivity.

3) The influence of the mixed inert gas species for plasma oxidization process of metallic Al layer on the tunnel magnetoresistance is investigated. By the use of $Kr-O_2$ plasma for Al oxidation process, a 58.8% of MR ratio is obtained at room temperature after annealing the junction at 300 °C, while the achieved TMR ratio of the MTJ fabricated with usual $Ar-O_2$ plasma remains 48.4%. A faster oxidization rate of the Al layer by using $Kr-O_2$ plasma is a possible cause to oxidize the Al layer homogeneously and prevent the over oxidization of Al layer partially, which decreases the MR ratio because of the depolarization of underlaid ferromagnetic layer.

References

[1] T. Miyazaki and N. Tezuka, J. Magn. Magn. Mater. **139**, L231 (1995).
[2] J. S. Moodera, L. R. Kinder, T. M. Wong, and R. Meservey, Phys. Rev. Lett. **74**, 3273 (1995).
[3] J. C. Slonczewski, Phys. Rev. B **39**, 6995 (1989).
[4] Y. Ando, H. Kubota *et al.*, Jpn. J. Appl. Phys. **39**, 5832 (2000).
[5] S. S. P. Parkin, K. P. Roche *et al.*, J. Appl. Phys. **85**, 5828 (1999).
[6] H. Kikuchi, M. Sato, and K. Kobayashi, J. Appl. Phys. **87**, 6055 (2000).
[7] S. Cardoso, P. P. Freitas, C. de Jesus, P. Wei, and f J. C. Soares, Appl. Phys. Lett. **76**, 610 (2000).
[8] X. F. Han, M. Oogane, H. Kubota, Y. Ando, and T. Miyazaki, Appl. Phys. Lett. **77**, 283 (2000).
[9] J. Watanabe, Y. Kawai, N. Konishi, and T. Ohmi, Jpn. J. Appl. Phys. **34**, 900 (1995).
[10] E. L. Wolf, Principles of Electron Tunneling Spectroscopy. Oxford, Oxford University Press, 1985.
[11] J. Zhang and R. M. White, J. Appl. Phys. **83**, 6512 (1998).
[12] T. Ueno, A. Morioka, S. Chikamura, and Y. Iwasaki, Jpn. J. Appl. Phys. **39**, L327 (2000).
[13] K. Sekine, Y. Saito, M. Hirayama, and T. Ohmi, IEEE Trans. Electron Devices **48**, 1550 (2001).
[14] J. S. Moodera, L. R. Kinder, J. Nowak, P. LeClair, and R. Meservey, Appl. Phys. Lett. **69**, 708 (1996).
[15] N. Goto and M. Yamamoto, Inst. Electr. Commun. Eng.

Tech. Rep. **AP80-57**, 43 (1980) [in Japanese].
[16] T. Yamamoto, N. T. Chien, M. Ando, N. Goto, M. Hirayama, and T. Ohmi, Jpn. J. Appl. Phys. **38**, 2082 (1999).
[17] Y. Saito, K. Sekine, M. Hirayama, and T. Ohmi, Jpn. J. Appl. Phys. **38**, 2329 (1999).
[18] T. Ohmi, S. Sugawa, M. Hirayama, and Y. Saito, OYO BUTURI **69**, 1200 (2000) [in Japanese].
[19] K. Nishikawa, M. Tsunoda, S. Ogata, and M. Takahashi, IEEE Trans. Magn. (submitted).
[20] J. G. Simmons, J. Appl. Phys. **34**, 1793 (1963).
[21] J. J. Åkerman, J. M. Slowghter, R. W. Dave, and I. K. Schuller, Appl. Phys. Lett. **79**, 3104 (2001).
[22] M. Tsunoda, K. Nishikawa, S. Ogata, and M. Takahashi, Appl. Phys. Lett. **80**, 3135 (2002).
[23] T. Ueno, T. Akiyama, K. Kuroiwa, and Y. Tarui, Appl. Surf. Sci. **79/80**, 502 (1994).
[24] M. Sato, H. Kikuchi, and K. Kobayashi, J. Appl. Phys. **83**, 6691 (1998).
[25] J. J. Sun, V. Soares, and P. P. Freitas, Appl. Phys. Lett. **74**, 448 (1999).